JOURNAL OF CHEMICAL & ENGINEERING DATA

ARTICLE

pubs.acs.org/jced

Comparative Studies of Removal of Cr(VI) and Ni(II) from Aqueous Solutions by Magnetic Nanoparticles

Y. C. Sharma* and V. Srivastava

Department of Applied Chemistry, Institute of Technology, Banaras Hindu University, Varanasi 221 005, India

ABSTRACT: Nanoscale iron particles are increasingly attracting interest as efficient sorbents for various types of pollutants from aqueous solutions and effluents. In the present study, nanoparticles were prepared by a coprecipitation method and then characterized by X-ray diffraction, transmission electron microscopy, Fourier transformation IR spectroscopy, and vibrating sample magnetometry. The diameters of the nanoparticles were in the range (10 to 15) nm. The adsorption of Ni(II) and Cr(VI) from diluted aqueous solutions onto Fe_3O_4 nanoparticles was investigated. The parameters studied include contact time and concentration of the metal ions. Iron nanoparticles demonstrated very rapid uptake of these metal ions. The adsorption was found to be highly dependent on solution pH. Cr(VI) removal was found to be greater in the acidic range while Ni(II) removal was greater in the basic range of solutions. Increasing the temperature increased the removal of both metal ions, indicating the endothermic nature of the system. Langmuir and Freundlich isotherm constants were determined and revealed that magnetic nanoparticles can serve as efficient adsorbents for the removal of Ni(II) and Cr(VI). These data can be used in the design of a treatment plant on an industrial scale.

1. INTRODUCTION

The major source of metallic pollutants in aquatic systems is discharge of untreated industrial effluents from different industries such as electroplating, dyeing, battery manufacturing, mining operations, chemical manufacturing, tanneries, glass manufacture, and pharmaceutical industries.[1−4] The metals, namely, chromium, cadmium, arsenic, nickel, zinc, copper, lead, and mercury, are regularly used in various industries. Their toxicities are well-documented.

Recently, low-cost materials having a high surface area for adsorption, such as iron oxide, aluminum oxide, and titanium oxide, have been used for removal of metallic pollutants from aqueous solutions and industrial effluents. Through the use of nanotechnology, highly efficient, low-cost materials can be prepared. Nanotechnology is basically the art, science, and engineering of manipulating objects on the (1 to 100) nm scale. It involves the design, synthesis, manipulation, characterization, and exploitation of materials and devices with structures defined in terms of nanometers.[5] Nanotechnology is an enabling technology that could potentially lead to cost-effective and high performance in water treatment systems. On the nanoscale, materials show unique characteristics, and because of their small size, they possess a large surface area and surface-area to volume ratio.[6] In addition to large surface area, these particles show unique characteristics, such as catalytic potential and high reactivity, that make them better adsorbing materials than conventional materials. Because of their large surface area, nanoparticles have a greater number of active sites for interaction with different chemical species. In the area of water purification, nanotechnology offers the possibility of efficient removal of pollutants. Because of their high efficiency, nanoparticles are becoming new alternatives to traditional adsorbents. Numerous studies have demonstrated that bulk iron oxides have good efficiency for removal of heavy metals from aqueous solutions. However, because of their high surface area, nanoparticles have better efficiency than bulk particles of the same material.[4] In spite of being noncorrosive, magnetic nanoparticles can easily be recovered by an external magnetic field.

In the present work, the removal of two metal ions, namely, Ni(II) and Cr(VI), from aqueous solution by synthesized magnetic iron nanoparticles was studied. Batch experiments were conducted to determine the effect of contact time, initial concentration, temperature, and pH on the removal of chromium and nickel from their aqueous solutions.

2. MATERIALS AND METHODS

All of the chemicals used were analytical-grade. Chemicals used in this study were ferrous chloride, ferric chloride, ammonia solution, acetone, potassium dichromate, 1,5-diphenylcarbazide, hydrochloric acid, sulfuric acid, sodium hydroxide, phosphoric acid, nickel sulfate, dimethylglyoxime, ethyl alcohol, and bromine.

2.1. Synthesis and Characterization of the Adsorbent. Magnetic nanoparticles were prepared by coprecipitation of Fe^{2+} and Fe^{3+} salts from aqueous solution using ammonia solution. A 2:1 molar ratio of ferric chloride and ferrous chloride was used in the preparation. A solution of Fe^{2+} and Fe^{3+} was prepared by dissolving the chlorides in distilled water. This solution was then heated to 40 °C for 10 min, after which the black-colored nanoparticles were precipitated by addition of ammonia solution with continuous stirring on a magnetic stirrer at 40 °C. These nanoparticles were then separated from the solution using a strong magnet and washed several times with distilled water and then with dilute HCl to remove the excess OH^-. Finally, the

Special Issue: John M. Prausnitz Festschrift

Received: April 27, 2010
Accepted: August 21, 2010
Published: October 07, 2010

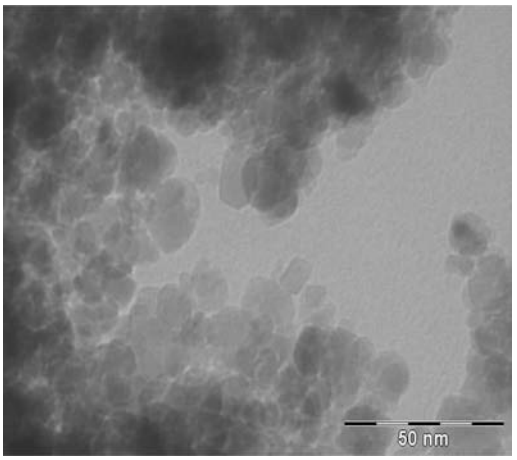

Figure 1. TEM image of the magnetic nanoparticles.

nanoparticles were washed with acetone, dried overnight in a hot-air oven at 60 °C, and then characterized using X-ray diffraction (XRD). The crystallite size was determined from the diffraction peaks using the Scherer formula:[7]

$$D = \frac{K\lambda}{w \cos \theta} \quad (1)$$

where D is the crystallite size (nm), λ is the wavelength of the monochromatic X-ray beam (0.154056 nm for Cu Kα radiation), w is the full width at half-maximum for the diffraction peak under consideration (rad), K is a constant (equal to 0.9), and θ is the diffraction angle (deg). For accurate determination of the lattice parameters, a JCPDS database[8] was used. Fourier transform IR (FTIR) spectra of Fe_3O_4 were obtained using an FTIR spectrometer (Shimadzu/84S, Japan). The sample was ground with 200 mg of KBr in a mortar and pressed into 10 mm diameter disks at a pressure of 10 tons under high vacuum for FTIR analysis. The Brunauer−Emmett−Teller (BET) surface area, pore volume, and pore size distribution were investigated using a computer-controlled automated porosimeter (Micromeritics ASAP 2020, V302G single port). The magnetic properties of the prepared iron nanoparticle powder were measured by using a vibrating sample magnetometer (model 73504, Lake Shore Cryotronics, Westerville, OH).

2.2. Metal Adsorption Experiments. Batch studies to measure the performance of the magnetic nanoparticles were conducted. For batch experiments, iron nanoparticles (4 g·L^{-1}) were mixed in simulated solutions of Ni(II) and Cr(VI). The ion concentrations were varied over the range from (5 to 15) mg·L^{-1} at 25 °C. The pH of the solutions was adjusted by adding dilute HCl or NaOH. The ionic strength of the aqueous solutions was maintained at $1.0 \cdot 10^{-2}$ M $NaClO_4$. After the equilibrium time, the adsorbent was separated from the solution by centrifugation at 10 000 rpm for 10 min. The residual concentration of Ni(II) in the solution was determined by UV−vis spectrophotometry at 445 nm, and the residual concentration of Cr(VI) was determined at 540 nm with 1,5-diphenylcarbazide following APHA and AWWA standard methods.[9] The amount of metal ions adsorbed per unit mass of the adsorbent was determined using the following equation:

$$Q = \left(\frac{C_i - C_e}{W}\right) V \quad (2)$$

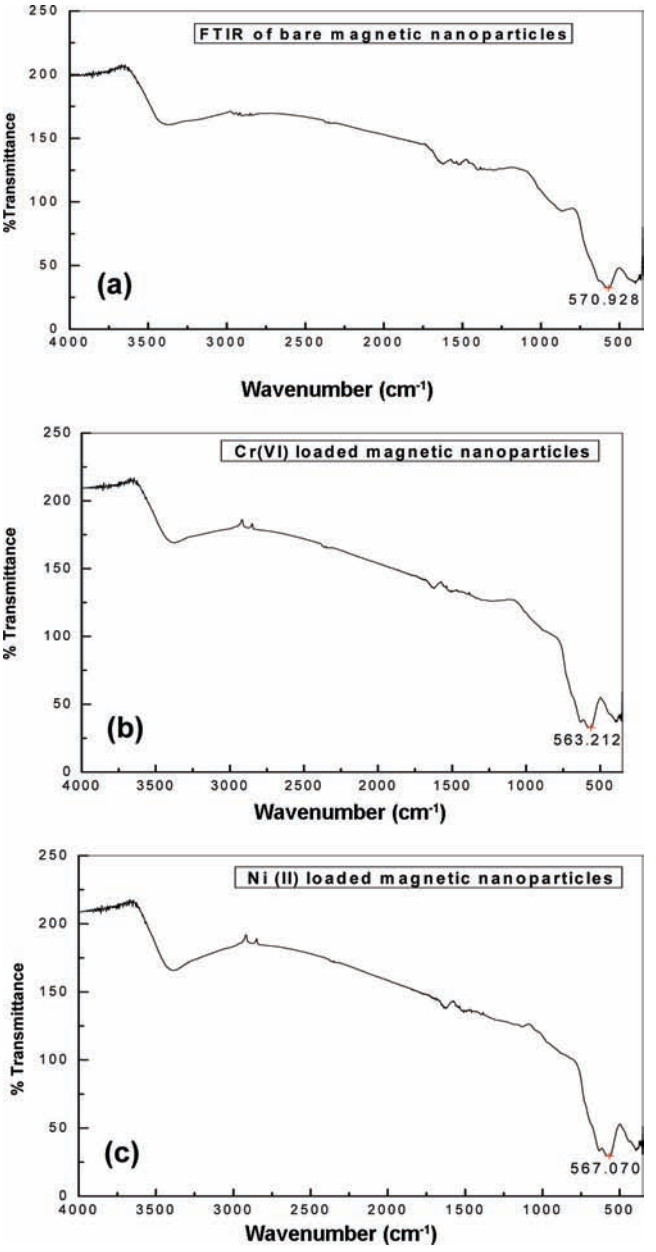

Figure 2. FTIR spectra of (a) magnetic nanoparticles synthesized by a coprecipitation method, (b) magnetic nanoparticles loaded with Cr(VI) ions, and (c) magnetic nanoparticles loaded with Ni(II) ions.

where Q is the amount of selected metallic species adsorbed per unit mass of the adsorbent (mg·g^{-1}), C_i and C_e are the initial and equilibrium concentrations, respectively (mg·L^{-1}), W is the mass of adsorbent (g), and V is the volume of solution (L). The percent removal of metal ions was calculated using the following equation:

$$\% \text{ removal} = \left(\frac{C_i - C_e}{C_i}\right) \cdot 100 \quad (3)$$

3. RESULTS AND DISCUSSION

3.1. Characterization of the Adsorbent. XRD analysis of the prepared sample revealed the formation of Fe_3O_4. The peaks

dx.doi.org/10.1021/je100428z |J. Chem. Eng. Data 2011, 56, 819–825

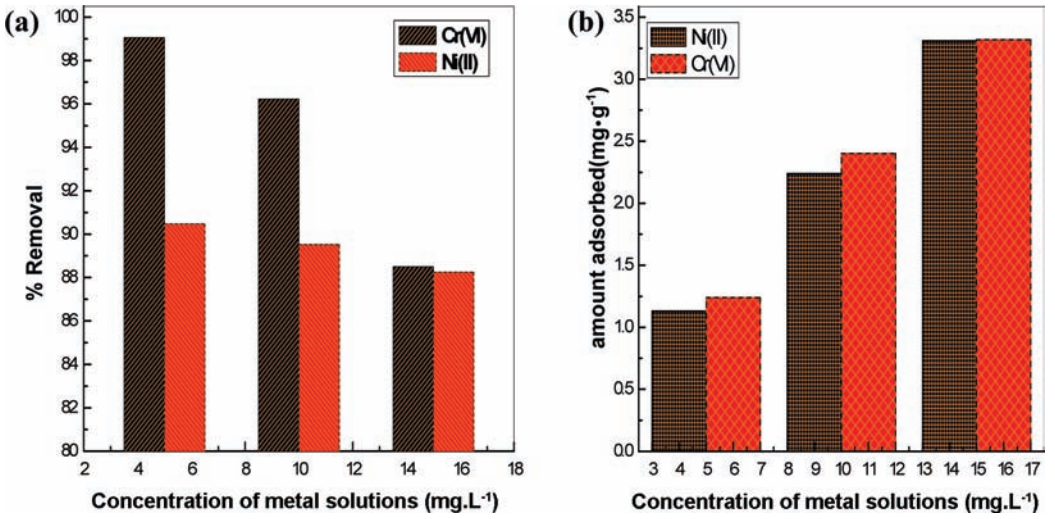

Figure 3. Effect of initial concentration: (a) percent removal of metal ions; (b) amount adsorbed on the adsorbent. Temperature, 298 K; nanoparticle dose, 4 $g \cdot L^{-1}$; 100 rpm.

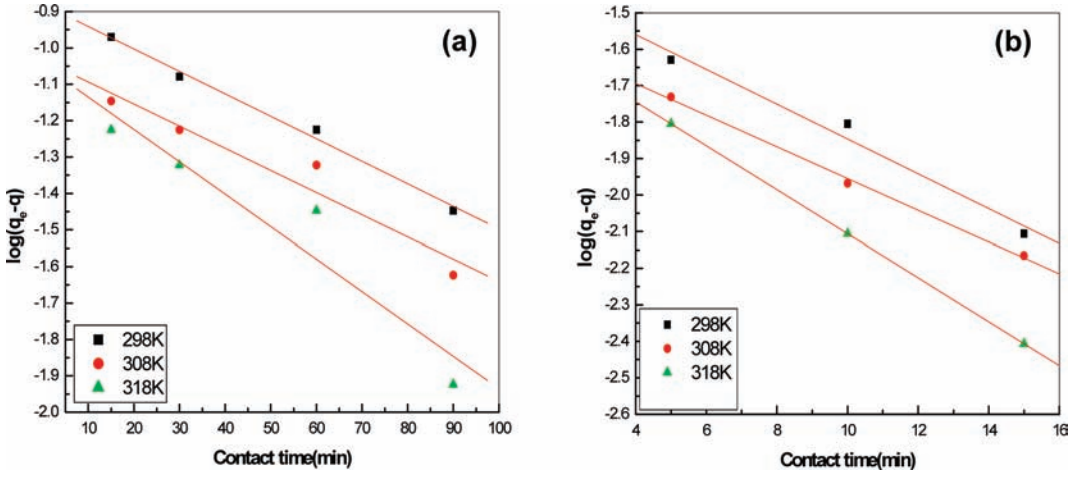

Figure 4. Lagergren plots for the removal of (a) Ni(II) and (b) Cr(VI).

were confirmed by comparison to JCPDS data (19-0629). The broad diffraction peaks confirmed the formation of small-sized particles (figure not shown). TEM images of the magnetic particles confirmed their nanoscale size in the prepared powder (Figure 1). The FTIR spectrum of the bare magnetic nanoparticles is shown in Figure 2a. The presence of peaks in the (3000 to 3500) cm^{-1} region is related to the lattice of water molecules, indicating the presence of moisture in the powder or KBr. The peak near 570 cm^{-1} is due to Fe−O functional groups. This peak is very sharp and has strong intensity, indicating the crystallinity of the sample. The FTIR spectra of magnetic nanoparticles loaded with Cr(VI) and Ni(II) were also measured (Figure 2b,2c) and clearly showed that after adsorption of metal ions, there was no significant change in the Fe−O peak. This suggested that chemical bonding between the metal ions and the nanoparticles plays no role in the adsorption and thus confirmed that removal of the metal occurs by physical adsorption. The BET surface area of the prepared nanoparticles was measured to be 86.55 $m^2 \cdot g^{-1}$. The saturation magnetization (M_s) of the sample was measured to be 55.26 emu $\cdot g^{-1}$ at room temperature. The remanence (M_r) and coercive force were found to be 1.2043 emu $\cdot g^{-1}$ and 12.191 G, respectively.

3.2. Effect of Initial Concentration on the Removal of Metal Ions from Aqueous Solutions. The effect of initial concentration on the removal of Cr(VI) and Ni(II) by adsorption on magnetic nanoparticles was studied. The concentration range selected for studies was (5 to 15) $mg \cdot L^{-1}$. The results obtained are plotted in Figure 3a,b as percent removal and amount adsorbed ($mg \cdot g^{-1}$) versus initial concentration, respectively. It is clear from Figure 3a that increasing the initial concentration decreased the percent removal from (99.1 to 88.5) % for Cr(VI) and (90.5 to 88.3) % for Ni(II) ions. Figure 3b shows that increasing the initial concentration of the adsorbate increased the amount adsorbed from (1.13 to 3.30) $mg \cdot g^{-1}$ for Cr(VI) and (1.23 to 3.31) $mg \cdot g^{-1}$ for Ni(II). Apparently, the initial concentration of the metal ion plays an important role and affects the adsorption capacity of metal ions on the adsorbent. This finding has industrial importance, as in most cases, lower concentrations of adsorbates and pollutants are encountered in real-life systems.

3.3. Kinetic Studies. Several models for the kinetic studies on the removal of nickel and chromium by iron nanoparticles were tried, but the only one that was applicable to both systems was Lagergren's model. Thus, the kinetic modeling of the removal of

dx.doi.org/10.1021/je100428z |J. Chem. Eng. Data 2011, 56, 819–825

Table 1. Values of the Lagergren Constants (k_{ad}) for Ni(II) and Cr(VI) Removal by Magnetic Nanoparticles and Corresponding Correlation Coefficients (as R^2)

	Ni(II) removal		Cr(VI) removal	
T/K	k_{ad}/min^{-1}	R^2	k_{ad}/min^{-1}	R^2
298	0.014	0.99	0.10	0.99
308	0.015	0.94	0.11	0.99
318	0.021	0.91	0.138	1.00

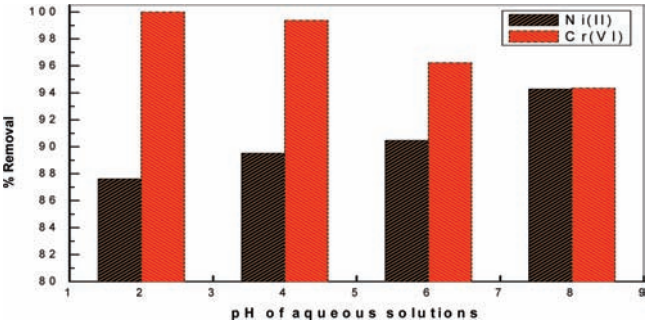

Figure 5. Effect of pH on metal removal. Ion concentration, 5 mg·L^{-1}; temperature, 298 K; nanoparticle dose, 4 g·L^{-1}; 100 rpm; pH range, 2.0 to 8.0.

Ni(II) and Cr(VI) by magnetic nanoparticles was carried out using Lagergren's model:[10]

$$\log(q_e - q) = \log q_e - \left(\frac{k_{ad}}{2.303}\right)t \quad (4)$$

where q and q_e (both mg·g^{-1}) are the amounts of metal ion adsorbed at a particular time and at equilibrium, respectively, and k_{ad} (min^{-1}) is the rate constant for adsorption. The straight-line plots of $\log[(q_e - q)]$ versus t (Figure 4a,b) confirmed that the process of removal is governed by first-order kinetics. The values of k_{ad} at various temperatures were obtained from the slopes of the corresponding plots (Figure 4a,b). The values of the rate constant at different temperatures for Ni(II) and Cr(VI) are given in Table 1. The linear plots also demonstrate the applicability of Lagergren's model to this study.

3.4. Effect of pH on Removal of Metal Ions from Aqueous Solutions. The solution pH has been recognized as one of the important parameters affecting the removal of a solute from the solution and has been termed a "master variable". The effect of pH on removal of Cr(VI) and Ni(II) is presented in Figure 5, which shows that the removal is highly dependent on the solution pH. The removal was high in the acidic range, with a maximum of 100 % at pH 2.0, and low in the alkaline range, with a minimum of 94.4 % at pH 8.0 for Cr(VI).

Different Cr(IV) species that commonly exist in aqueous solution are $Cr_2O_7^{2-}$, $HCrO_4^-$, CrO_4^{2-}, and $HCr_2O_7^-$. Removal of Cr(VI) from aqueous solution decreased with increasing pH from 2.0 to 8.0. Similar findings have also been reported by other investigators.[11] It may be due to the presence of more H^+ ions at lower pH. At lower pH, $HCrO_4^-$ is the major species, as OH^- groups are neutralized by hydrogen ions, favoring the adsorption of this species. At higher pH, $Cr_2O_7^{2-}$ and CrO_4^{2-} are present in aqueous solution. In this condition, the presence of a larger number of OH^- groups hinders the diffusion

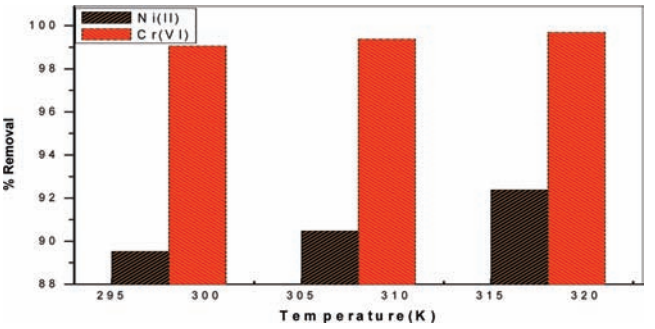

Figure 6. Effect of temperature on percent removal of metal ions. Ion concentration, 5 mg·L^{-1}; temperature, (298 to 318) K; nanoparticle dose, 4 g·L^{-1}; 100 rpm.

of dichromate ions, causing the percent removal to decrease with increasing pH.

In the case of Ni(II), the adsorption increased from (87.6 to 94.3) % as the pH of solution was increased from 2.0 to 8.0. Ni^{2+} is the only important oxidation state in the aqueous chemistry of nickel, and this species is prominent up to pH 8.0. It is present in aqueous solutions as $Ni(H_2O)_6^{2+}$.[12] At pH >8.0, Ni(II) precipitates as $Ni(OH)_2$ because of the presence of hydroxide anions.[13,14] The protonated surface favors the adsorption of Ni(II) from aqueous solution. The following hydrolysis and adsorption reactions are expected at the solid (S)−solution interface:[10]

$$H{-}OH + M^{z+} \rightleftarrows H{-}OM^{(z-1)+} + H^+ \quad (5)$$

$$S{-}OH + M^{z+} \rightleftarrows S{-}OM^{(z-1)+} + H^+ \quad (6)$$

The metal competes with protons for surface sites:

$$S{-}OH + Ni^{2+} \rightleftarrows S{-}O{-}Ni^{2+} + H^+ \quad (7)$$

It appears that during adsorption one proton is replaced by one nickel ion.

The removal of chromium in both pH ranges can also be explained on the basis of the following complex reactions:

$$\text{lower pH}: \quad S{-}OH + HCrO_4^- \rightleftarrows S{-}HCrO_4 + OH^- \quad (8)$$

$$\text{higher pH}: \quad S{-}OH + CrO_4^{2-} \rightleftarrows S{-}CrO_4^- + OH^- \quad (9)$$

3.5. Effect of Temperature on Removal of Metal Ions from Aqueous Solutions. The effect of temperature on Ni(II) and Cr(VI) removal from aqueous solutions is presented in Figure 6, which shows that the removal percentages of both metal ions increased with increasing temperature from (298 to 318) K. Higher temperatures favor adsorption of both metal ions, which reveals the endothermic nature of adsorption of metal ions on iron nanoparticles. An increase in removal can be explained in terms of an increase in the number of active sites with increasing temperature due to some breakage of bonds near active sites.

3.6. Adsorption Isotherm Study. To investigate the relationship between the adsorbed species and their equilibrium concentrations, the Langmuir and Freundlich isotherms were applied to the generated data.

3.6.1. Langmuir Isotherm. The Langmuir isotherm is applicable to adsorption on homogeneous surfaces. According to this

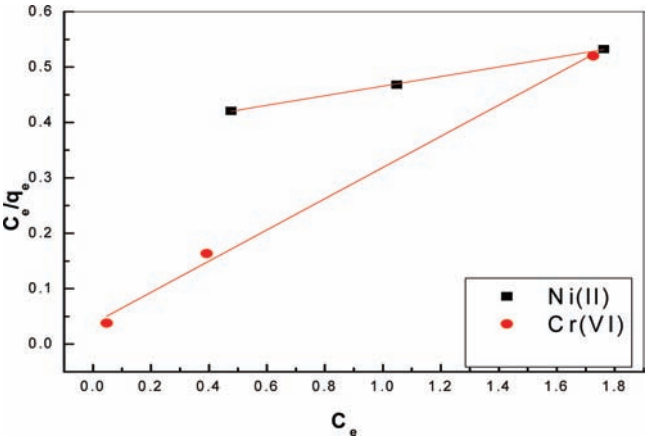

Figure 7. Langmuir plots for Ni(II) and Cr(VI) removal by magnetic nanoparticles. Ion concentration, 5 mg·L^{-1}; temperature, 298 K; nanoparticle dose, 4 g·L^{-1}; 100 rpm.

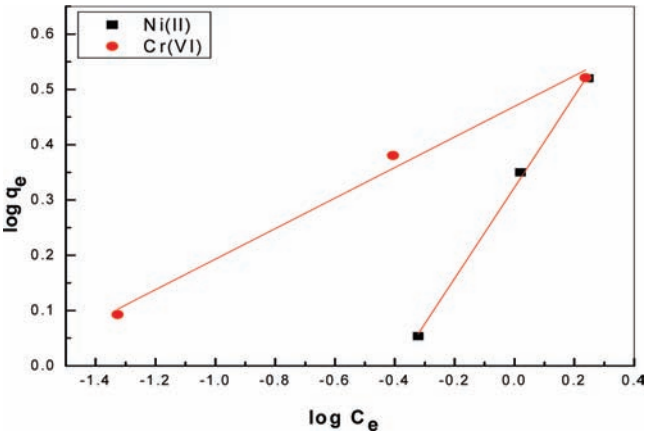

Figure 8. Freundlich plot for Ni(II) and Cr(VI) removal by magnetic nanoparticles. Ion concentration, 5 mg·L^{-1}; temperature, 298 K; nanoparticle dose, 4 g·L^{-1}; 100 rpm.

Table 2. Values of the Langmuir Constants $Q°$ and b for Adsorption of Ni(II) and Cr(VI) on Magnetic Nanoparticles at 298 K and the Corresponding Correlation Coefficients (as R^2)

ion	$Q°$/mg·g^{-1}	b/L·mg^{-1}	R^2
Ni(II)	11.53	0.228	0.999
Cr(VI)	3.55	7.578	0.996

isotherm, there is a constant number of available sites on the adsorbent surface. The linearized form of this isotherm can be expressed as follows:[10]

$$\frac{C_e}{q_e} = \frac{1}{Q°b} + \frac{C_e}{Q°} \tag{10}$$

where C_e (mg·L^{-1}) is the equilibrium concentration of the solute, q_e is amount adsorbed at equilibrium (mg·g^{-1}), and $Q°$ (mg·g^{-1}) and b (L·mg^{-1}) are constants related to the adsorption capacity and energy of adsorption, respectively. Values of the Langmuir constants $Q°$ and b were calculated from the slopes and intercepts, respectively, of plots of C_e/q_e versus C_e (Figure 7) and are given in Table 2. The values of $Q°$ and b for the removal of Ni(II) and Cr(VI) at 298 K were found to be (11.53 and 3.55) mg·g^{-1} and (0.228 and 7.578) L mg^{-1}, respectively.

3.6.2. Freundlich Isotherm. The Freundlich isotherm is based on a heterogeneous surface. It can be expressed as follows:[10]

$$q_e = K_f C_e^{1/n} \tag{11}$$

where q_e is the amount adsorbed (mg·g^{-1}), C_e is the equilibrium concentration (mg·L^{-1}), and K_f and $1/n$ are related to the adsorbent capacity and sorption intensity of the adsorbent, respectively. Equation 11 can be linearized as follows:

$$\log q_e = \log K_f + \frac{1}{n}\log C_e \tag{12}$$

The values of the Freundlich constants K_f and n were determined from the intercepts and slopes, respectively, of the plots shown in Figure 8. The values of K_f for removal of Ni(II) and Cr(VI) from aqueous solutions at 298 K were found to be (2.10 and 2.94) mg·g^{-1}, and the n values were (1.21 and 3.62) L·g^{-1} respectively (Table 3).

Table 3. Values of the Freundlich Constants K_f and n for Adsorption of Ni(II) and Cr(VI) on Magnetic Nanoparticles at 298 K and the Corresponding Correlation Coefficients as (R^2)

ion	K_f/mg·g^{-1}	n/L·g^{-1}	R^2
Ni(II)	2.104	1.21	0.999
Cr(VI)	2.94	3.62	0.991

The adsorption capacities of various conventional adsorbents are listed in Table 4. It is clear from this table that the adsorption capacity of the prepared iron nanoparticles is significant in comparison with the other listed adsorbents.[15−30]

The R^2 values for the parameters of the two isotherm models were calculated, and these values suggest that both models fit the equilibrium data.

3.7. Thermodynamic Studies. Thermodynamic studies are used to explain any reaction in a better way. In the present investigations, thermodynamic studies were performed, and the values of the thermodynamic parameters $\Delta G°$, $\Delta H°$, and $\Delta S°$ were determined at (298, 308, and 318) K using the following equations:[10]

$$K_c = \frac{C_{ad}}{C_e} \tag{13}$$

$$\Delta G° = -RT \ln K_c \tag{14}$$

$$\Delta H° = R\left(\frac{T_2 T_1}{T_2 - T_1}\right) - \ln\left(\frac{K_{c1}}{K_{c2}}\right) \tag{15}$$

$$\Delta S° = \frac{\Delta H° - \Delta G°}{T} \tag{16}$$

where K_c is the equilibrium constant and C_{ad} and C_e are the equilibrium concentrations of metal ions on the adsorbent surface and in the solution, respectively. The values of $\Delta G°$, $\Delta H°$, and $\Delta S°$ for the removal of Ni(II) and Cr(VI) from their aqueous solutions determined at (298, 308, and 318) K are given in Table 5. The values of $\Delta G°$ and $\Delta H°$ at 298 K were found to be (−5.44 and 33.72) kJ·mol^{-1}, and the value of $\Delta S°$ at 298 K was 131.43 J·mol^{-1}·K^{-1}.

dx.doi.org/10.1021/je100428z |J. Chem. Eng. Data 2011, 56, 819–825

Table 4. Comparison of Ni(II) and Cr(VI) Adsorption Capacities of Some Conventional Adsorbents with Those of Magnetic Nanoparticles

Cr(VI)			Ni(II)		
adsorbent	capacity/mg·g^{-1}	ref	adsorbent	capacity/mg·g^{-1}	ref
riverbed sand	0.15	15	coir pith	9.5	23
coconut shell powder	1.23	16	granular activated carbon	1.49	24
wollastonite	0.83	17	sheep manure waste	7.20	25
fly ash	1.4	18	bituminous coal	6.47	26
activated alumina	1.6	19	bagasse	0.001	27
sawdust	3.6	20	calcium alginate	10.5	28
spent activated clay	1.5	11	fly ash	0.03	27
wheat bran	0.942	21	sphagnum moss peat	9.2	29
pine leaves	0.277	22	magnetic nanoparticles	11.53	this work
magnetic nanoparticles	3.56	this work	thuja orientalis	12.42	30

Table 5. Values of Thermodynamic Parameters at Various Temperatures

ion	T/K	$\Delta G°$/kJ·mol^{-1}	$\Delta H°$/kJ·mol^{-1}	$\Delta S°$/J·mol^{-1}·K^{-1}
Ni(II)	298	−5.44	33.72	131.43
	308	−6.78		
	318	−8.54		
Cr(VI)	298	−11.55	31.17	143.34
	308	−12.97		
	318	−15.23		

The positive value of the enthalpy change $\Delta H°$ also indicates the endothermic nature of the adsorption of Ni(II) and Cr(VI) on iron nanoparticles. Thermodynamic studies revealed that greater adsorption can be obtained at higher temperatures.

CONCLUSIONS

Magnetic nanoparticles are effective adsorbents for the removal of Ni(II) and Cr(VI) from aqueous solutions. The adsorption was found to be highly dependent on pH. Acidic conditions favor Cr(VI) removal, while Ni(II) removal was found to be greater under basic conditions. The percent removal of both metals was higher at lower concentration. Furthermore, the low particle-mass to solution ratio allows the process to compete with more traditional separation techniques. The adsorption data fit both the Langmuir and Freundlich isotherms well. Adsorption of Ni(II) and Cr(VI) increases with increasing temperature, indicating the endothermic process of the reaction. In both systems, higher temperatures favor removal of metal ions. The value of the enthalpy change further confirmed the endothermic nature of the adsorption reaction. All of the values of the Gibbs energy change were found to be negative, showing the spontaneous nature of the process of removal.

The nanoparticles prepared here are not very costly, and the resultant data can be useful for designing treatment plants for water enriched with Cr(VI) and Ni(II) ions, even by small-scale industries. The data generated pertain to aqueous solutions, and the behavior of the adsorbents must be examined for industrial effluents. The generated data can serve as baseline data for designing treatment plants for treatment of metal-rich wastewater in particular and of pollutant species in general.

AUTHOR INFORMATION

Corresponding Author

*E-mail: ysharma.apc@itbhu.ac.in. Tel.: +91 542 6702865.

REFERENCES

(1) Mukherjee, A. G. *Environmental Pollution and Health Hazards: Causes and Control*; Galgotia Publications: New Delhi, 1986.

(2) Nriago, J. O. A silent epidemic of metal poisoning. *Environ. Pollut.* **1988**, *50*, 139–161.

(3) Kanan, K. *Fundamentals of Environmental Pollution*, 1st ed.; S. Chand India: New Delhi. 1985.

(4) Förstner, U.; Wittmann, G. T. W. *Metals in the Aquatic Environment*; Springer: New York, 1985.

(5) Booker, R.; Boysen, E. *Nanotechnology for Dummies*; Wiley Publishing Inc.: Indianapolis, IN, 2005.

(6) Mamalis, A. G. Recent advances in nanotechnology. *J. Mater. Process. Technol.* **2007**, *181*, 52–58.

(7) You, H. J. C.; Song, Z.; Yu, B.; Shen, Y. Influences of different synthesis conditions on properties of Fe_3O_4 nanoparticles. *Mater. Chem. Phys.* **2009**, *113*, 46–52.

(8) *JCPDS Powder Diffraction File*; International Centre For Diffraction Data: Newtown Square, PA, 1997.

(9) *Standard Methods for the Examination of Water and Wastewater*, 14th ed.; APHA/AWWA: Washington, DC, 1975.

(10) Sharma, Y. C.; Srivastava, V.; Upadhyay, S. N.; Weng, C. H. Alumina nanoparticles for removal of the Ni(II) from aqueous solutions. *Ind. Eng. Chem. Res.* **2008**, *47*, 8095–8100.

(11) Weng, C. H.; Sharma, Y. C.; Chu, S. H. Adsorption of Cr(VI) from aqueous solutions by spent activated clay. *J. Hazard. Mater.* **2008**, *155*, 65–75.

(12) Stumm, W. *Aquatic Surface Chemistry*; Wiley-Interscience: New York, 1989.

(13) Panda, G. C.; Das, S. K.; Bandopadhyay, T. S.; Guha, A. K. Adsorption of nickel on husk of Lathyrus Sativus: behavior and binding mechanism. *Colloids Surf., B* **2007**, *57*, 135–142.

(14) Weng, C. H. Removal of nickel(II) from dilute aqueous solution by sludge-ash. *J. Environ. Eng.* **2002**, *128*, 716–722.

(15) Sharma, Y. C.; Weng, C. H. Removal of chromium(VI) from water and wastewater by using riverbed sand: Kinetic and equilibrium studies. *J. Hazard. Mater.* **2006**, *142*, 449–454.

(16) Pino, G. H.; Mesquita-De, L. M. S.; Torem, M. L.; Pinto, G. A. S. Biosorption of heavy metals by powder of green coconut shell. *Sep. Sci. Technol.* **2006**, *41*, 3141–3153.

(17) Sharma, Y. C. Effect of temperature on interfacial adsorption of Cr(VI) on wollastonite. *J. Colloid Interface Sci.* **2001**, *233*, 265–27.

(18) Banarjee, S. S.; Joshi, M. V.; Jayaram, R. V. Removal of Cr(VI) and Hg(II) from aqueous solutions using fly ash and impregnated fly ash. *Sep. Sci. Technol.* **2004**, *39*, 1611–1629.

(19) Bishnoi, N. R.; Bajaj, M.; Sharma, N.; Gupta, A. Adsorption of Cr(VI) on activated rice husk carbon and activated alumina. *Bioresour. Technol.* **2004**, *91*, 305–307.

(20) Baral, S. S.; Das, S. N.; Rath, P. Hexavalent chromium removal from aqueous solution by adsorption on treated sawdust. *Biochem. Eng. J.* **2006**, *31*, 216–222.

(21) Nameni, M.; Moghadam, A. M. R.; Armani, M. Adsorption of hexavalent chromium from aqueous solutions by wheat bran. *Int. J. Environ. Sci. Technol.* **2008**, *5*, 161–168.

(22) Morshedzadeh, K.; Soheilizdeh, H..R.; Zangoie, S.; Aliabadi, M. Removal of Cr(VI) from aqueous solutions by lignocellulosic solid waste. First Environment Conference, Department of Environment Engineering, Tehran University, 2007.

(23) Ewecharoen, A. P.; Nakbanpote, W. Comparison of nickel adsorption from electroplating rinse water by coir pith and modified coir pith. *Chem. Eng. J.* **2008**, *137*, 181–188.

(24) Perisamay, K.; Namasivayam, C. Removal of nickel(II) from aqueous solution and nickel plating industry wastewater using an agricultural waste: peanut hulls. *Waste Manage.* **1995**, *15*, 63–68.

(25) Alrub, F. A.; Kandah, M.; Aldabaibeh, N. Nickel removal from aqueous solutions by using sheep manure wastes. *Eng. Life Sci.* **2002**, *2*, 111–116.

(26) Singh, D.; Rawat, N. S. Adsorption of heavy metal ion on treated and untreated low-grade bituminous coal. *J. Chem. Technol. Biotechnol.* **1997**, *63*, 39–41.

(27) Rao, M.; Parwate, A. V.; Bhole, A. G. Removal of Cr^{6+} and Ni^{2+} from aqueous solution using bagasse and flyash. *Waste Manage.* **2002**, *22*, 821–830.

(28) Huang, C.; Chien, C. Y.; Ren, L. M. Adsorption of Cu(II) and Ni(II) by pelletized biopolymer. *J. Hazard. Mater.* **1996**, *45*, 265–267.

(29) Ho, Y. S.; Wase, D. A. J.; Forster, C. F. Batch nickel removal from aqueous solution by Sphagnum moss peat. *Water Res.* **1978**, *29*, 505–512.

(30) Malkoc, E. Ni(II) Removal from Aqueous Solutions Using Cone Biomass of Thuja Orientalis. *J. Hazard. Mater.* **2006**, *137*, 899–908.